Interaction of Carboxylate Inhibitors with the Active Site of Nickel(II) Carboxypeptidase A

José-María Moratal,* Josep Castells, Antonio Donaire, Jesús Salgado and Hermas R. Jiménez
Department of Inorganic Chemistry, University of Valencia, C/Dr. Moliner 50, 46100 Burjassot (Valencia), Spain

The binding of several carboxylate inhibitors to nickel(II)-substituted carboxypeptidase A, NiCPA, has been investigated through ^1H, ^{13}C NMR and electronic absorption spectroscopies. Both β-phenylpropionate and phenylacetate interact with NiCPA forming two complexes of stoichiometries 1:1 and 1:2 and their affinity constants were determined. Whereas the first inhibitor molecule binds at a non-metallic site, the second binds directly to the metal ion in slow exchange on the chemical shift time-scale. Proton nuclear Overhauser effect measurements have been performed on the 1:2 β-phenylpropionate complex, allowing a full correlation between the isotropically shifted signals. From the ^1H T_1 values of the *meta*-like protons of the co-ordinated histidines and the molar absorbances of the 1:2 complexes formed, five-co-ordination for the nickel ion is suggested. The NMR data indicate that upon binding of the carboxylate to the metal ion a conformational change occurs. In contrast, acetate displays no evidence for more than a single binding mode to the nickel enzyme. Thus ^1H and ^{13}C NMR data indicate that acetate binds to the metal ion forming a 1:1 complex in a fast-exchange regime. The Ni • • • ^{13}C distance, r = 2.7 Å, calculated by means of the Solomon equation, is consistent with direct co-ordination of the acetate to the metal ion.

The zinc metalloenzyme carboxypeptidase A, CPA, is an exopeptidase, of molecular weight 34 742, which catalyses the hydrolysis of C-terminal amino acids from polypeptide substrates.[1,2] The pancreatic bovine enzyme has been extensively studied and it serves as the prototypic zinc protease.[3–6] The crystal structure of the native enzyme has been refined at a resolution of 1.54 Å and the catalytic zinc ion is co-ordinated to two imidazole groups from His-69 and His-196, to a carboxylate bidentate group from Glu-72 and to a water molecule.[7]

Nickel(II) has been used as a probe to monitor the structure and reactivity of several zinc enzymes such as carbonic anhydrase, liver alcohol dehydrogenase and carboxypeptidase.[8–12] The nickel(II)-substituted carboxypeptidase, NiCPA, retains practically completely the enzymatic activity[13] and its structure has been determined by X-ray crystallography.[14] The metal ion is bound to the same residues as in the native enzyme and the ligand stereochemistry is close to square pyramidal which was described as octahedral minus one ligand.[14]

Key functional groups for binding and catalysis in the carboxypeptidase A active site include several cationic groups such as Arg-145, Arg-127 or Arg-71. Its substrates contain negatively charged terminal carboxylates. Consequently, much attention has been devoted to the study of CPA adducts with inhibitors such as D- and L-amino acids as well as carboxylate anions in order to elucidate their modes of binding to the protein.[15–19] The X-ray structures of CPA adducts with several inhibitors or substrate analogues invariably show that the terminal carboxylate binds Arg-145.[20–22]

Recent spectroscopic studies have shown that the binding to CoCPA of L- or D-amino acids as well as small anionic carboxylate-containing inhibitors allows the access of such anions to the metal co-ordination sphere. Whereas the cobalt enzyme has been extensively used in these investigations, studies on NiCPA have been very scarce.

We recently studied the nickel(II) carboxypeptidase and its interaction with the amino acids L- and D-phenylalanine as well as the formation of ternary complexes with these amino acids and azide.[23] Furthermore, we have investigated the interaction of NiCPA with phosphate and pyrophosphate as well as the effect on this interaction of the binding of an amino acid in the non-metallic S'_1 site.[24] Proton NMR spectroscopy of isotropically shifted signals for these NiCPA complexes is a useful tool for detecting structural changes within the active site of the enzyme.

We present herein the results of a comprehensive study of the interaction between NiCPA and carboxylate inhibitors such as β-phenylpropionate, phenylacetate and acetate. The structural and thermodynamic characteristics of these complexes have been investigated using UV/VIS, ^1H and ^{13}C NMR spectroscopies. Furthermore we performed ^1H nuclear Overhauser effect (NOE) measurements in order to assign vicinal proton pairs and correlate the resonances corresponding to CH_2 groups.

Experimental

Bovine carboxypeptidase A, prepared by the method of Cox *et al.*,[25] was purchased from Sigma and further purified through affinity chromatography on CABS-Sepharose to remove protease contaminants.[26,27] The nickel(II) derivative was prepared through zinc removal by the published procedure.[28,29] Standard precautions were taken to remove adventitious metal ions from all solutions.[23,30] The enzyme concentration was determined at 278 nm by using a molar absorption coefficient of 6.4×10^4 dm^3 mol^{-1} cm^{-1}.[31] The formation of NiCPA could be monitored by electronic and ^1H NMR spectroscopies.[23] The compounds $NiSO_4 \cdot 6H_2O$, β-phenylpropionate, phenylacetate, acetate and all the other chemicals were Merck analytical grade reagents. The 99% $^{13}CO_2^-$-enriched phenylacetate and acetate were obtained from Sigma and the 99.7% D_2O from Fluka.

Near-infrared and visible absorption spectra were recorded on a UV/VIS-NIR Perkin Elmer Lambda 9 spectrophotometer, using microcells with an optical path length of 10 mm. Samples for spectrophotometric measurements were prepared in D_2O {1 mol dm^{-3} NaCl, 50×10^{-3} mol dm^{-3} hepes [*N'*-(2-hydroxyethyl)piperazine-*N*-ethanesulfonic acid], pD 7} and the NiCPA concentrations were approximately 1.0×10^{-3} mol dm^{-3}. The spectra were registered using as reference a solution of the native enzyme under the same conditions. The estimated

error in the ε values is about 10%. The pH values of all the solutions were measured on a Crison digit-501 pH meter provided with an Ingold combined microelectrode.

The samples for NMR measurements were concentrated to (1–4) × 10^{-3} mol dm^{-3} protein by ultrafiltration at 2–4 °C using a Centricon microconcentrator (Amicon) with a molecular weight cut-off of 10 000. The ^1H NMR spectra were recorded on a Bruker AC-200 MHz spectrometer at 10 and 20 °C (1 mol dm^{-3} NaCl, 50 × 10^{-3} mol dm^{-3} hepes, pH 7) using the SUPERWEFT[32] multipulse sequence, 180°–τ–90°–acquisition + delay, with τ values of about 90 and 83 ms recycle time. The use of such a sequence enables us selectively to reduce the intensity of signals with longitudinal relaxation times longer than those of signals of interest. Spectra typically consisted of *ca.* 16 000 scans with 8K data points and a spectral width of 50 kHz. Chemical shifts were measured from the H_2O or HDO signals and referenced to $SiMe_4$ assumed at −4.8 ppm from the water signal. A 20 Hz line-broadening function was applied to improve the signal-to-noise ratio. The spin–lattice relaxation times ^1H T_1 of the isotropically shifted signals were determined by measuring the intensity of the signals I_τ as a function of the time τ between subsequent pulses of the MODEFT sequence.[33] The data were best fitted using equation (1)[33] with a non-linear

$$I_\tau = I_0(1 - 2e^{-\tau/T_1} + e^{-2\tau/T_1}) \quad (1)$$

two-parameter best-fitting program to obtain I_0 and T_1 values. The estimated error was about 5%.

The ^1H NOE experiments were performed as already reported[34] by using the SUPERWEFT[32] multipulse sequence. The signals were selectively saturated by using a selective decoupling pulse, whose power was predetermined (less than 0.1 W), kept on for 19/20 of the τ value. Difference spectra were collected by applying the decoupler frequency on and off alternately following the scheme, ω, ω + Δω, ω, ω − Δω, where ω is the frequency of the irradiated signal and Δω is the offset for the off-resonance irradiation. The value of Δω depends on the linewidth of the irradiated signal and the proximity of other signals of interest; typically values of 100–400 Hz were used. For each final difference spectrum 80–90 blocks were collected, 8192 scans each. The magnitude of a NOE in each case was determined from the integrated intensities of the peaks of interest.

The ^{13}C NMR measurements were performed on a Bruker AC-200 MHz instrument at 10 and 20 °C, using a spectral width of 1.5 kHz with 8K data points and a 4 Hz line-broadening function. Longitudinal relaxation times T_1 were measured with the inversion-recovery method by using an appropriate non-linear least-squares-fitting program. The ^{13}C NMR transverse relaxation times, T_2, were obtained from the linewidth at half-height through the relation $T_2^{-1} = \pi\Delta\nu_{\frac{1}{2}}$.

Consider the particular case of two binding sites for the inhibitor in the protein and where the concentration of complexed sites is very low compared with the concentration of the free ligand. In the presence of a paramagnetic centre, and under rapid-exchange conditions, the total relaxation rate of the ^{13}C nucleus changes as in equation (2),[10] where T_{1d}^{-1} is the

$$T_1^{-1} = T_{1d}^{-1} + (f_1 + f_2)T_{1M(1)}^{-1} + f_2T_{1M(2)}^{-1} \quad (2)$$

intrinsic diamagnetic relaxation rate of the ^{13}C nucleus, and $T_{1M(1)}^{-1}$ and $T_{1M(2)}^{-1}$ are the rate enhancements in the respective sites by the nearby paramagmetic centre. The molar fractions of bound inhibitor f_1 and f_2 are given by $f_1 = [EI]/I_t$ and $f_2 = [EI_2]/I_t$, where I_t is the total inhibitor concentration and [EI] and [EI_2] are the concentrations of the 1:1 and 1:2 complexes respectively.

Results

Electronic Spectra.—The absorption spectra in the range 360–1000 nm of nickel(II)-substituted carboxypeptidase (NiCPA) and its adducts with β-phenylpropionate and phenylacetate at pH 7 and 10 °C are shown in Fig. 1. The spectrum of NiCPA displays three absorption bands at 412(24), 685(7) and ≈1060 nm (ε ≈ 4 dm^3 mol^{-1} cm^{-1}) in agreement with reported values.[35] When β-phenylpropionate or phenylacetate is added to a solution of NiCPA the optical spectrum of the nickel enzyme undergoes marked changes. Both visible absorption bands are red shifted and enhanced in intensity. Thus, the visible spectrum of the phenylacetate complex shows two main absorption bands at 420 (ε = 44) and 705 nm (ε = 14 dm^3 mol^{-1} cm^{-1}). The electronic spectrum of the β-phenylpropionate adduct has already been reported,[35] and it is very similar to that of the phenylacetate. Indeed, it displays two bands at 427(54) and 705 nm (ε = 15 dm^3 mol^{-1} cm^{-1}), that have been analysed assuming a five-co-ordinated symmetry for the nickel ion.[35]

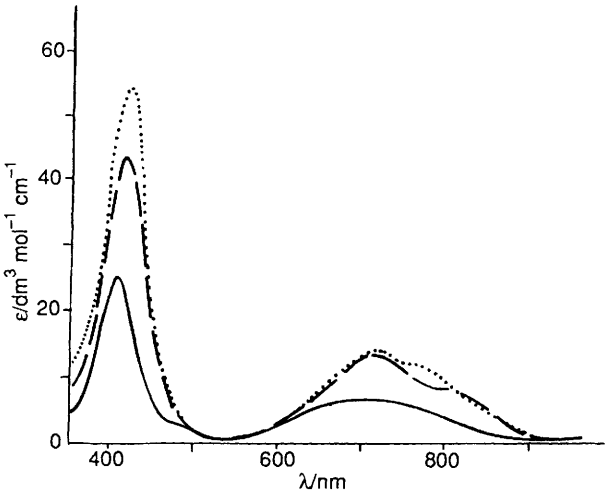

Fig. 1 Electronic absorption spectra of NiCPA (——) and its adducts with β-phenylpropionate (· · · ·) and phenylacetate (– – – –) at pH 7 (0.05 mol dm^{-3} hepes, 1 mol dm^{-3} NaCl) and 10 °C

^1H NMR Spectra.—As previously reported,[24] the ^1H NMR spectrum of NiCPA at pH 7 displays, in the downfield region, three resolved paramagnetically shifted signals at δ 57.5 (a), 53.3 (c) and 48.9 (d) [Fig. 2(*a*)]. In D_2O only signal a disappears in agreement with the previous assignment of this signal to a co-ordinated histidine NH(ε2). The other sharp signals, c and d, are assigned to the HC(δ2) protons of the two co-ordinated histidines, His-69 and -196 (Scheme 1). The second NH histidine is missing in the ^1H NMR spectrum and it has been suggested that it exchanges rapidly with bulk water on the NMR time-scale.[23]

The ^1H NMR spectrum of NiCPA is not sensitive to the addition of β-phenylpropionate up to concentrations as large as 1.6 × 10^{-3} mol dm^{-3}. For higher β-phenylpropionate concentrations drastic changes are produced in the spectrum, and the variation is practically complete at 10^{-2} mol dm^{-3}. Whereas the signals of NiCPA disappear progressively, a new set of four resolved signals at δ 65.6 (a′), 55.1 (d′), 50.8 (c′) and 49.0 (b′) appear as can be observed in the ^1H NMR titration (Fig. 3). In addition, two broad signals at δ 60 (e) and 22 (f) as well as a poorly defined signal about δ 46 can also be observed. This behaviour is typical of slow exchange on the NMR time-scale between free and bound β-phenylpropionate. The signals a′ and b′ are exchangeable, allowing them to be assigned to the NH(ε2) protons of the two co-ordinated histidines. The non-exchangeable signals d′ and c′ are assigned to the HC(δ2) of the same histidines according to the NOE experiments (see below).

The spectral behaviour of β-phenylpropionate can be explained by assuming the stepwise formation of two complexes of stoichiometries 1:1 and 1:2, NiCPA(β-phenylpropionate) and NiCPA(β-phenylpropionate)$_2$. The first inhibitor moiety does not alter the nickel(II) stereochemistry and binds at a non-

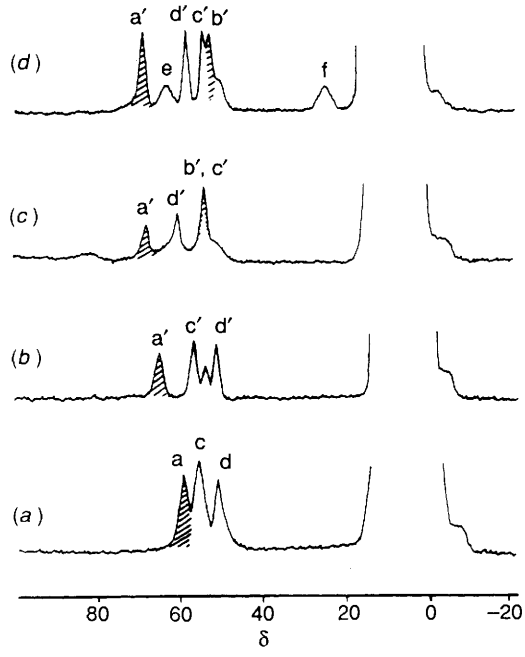

Fig. 2 Proton NMR spectra of NiCPA (*a*), and its adducts with acetate (*b*), phenylacetate (*c*) and β-phenylpropionate (*d*). Shaded signals disappear in D_2O. Solution conditions: (1.5–3) × 10^{-3} mol dm^{-3}, pH 7 and 20 °C

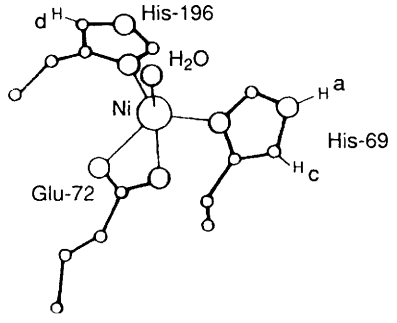

Scheme 1

metallic site. However, the second β-phenylpropionate molecule produces marked changes in the ^1H NMR spectrum and it can be proposed that the carboxylate group of β-phenylpropionate binds to the metal site.

From the normalized area of signal a′ as a function of increasing β-phenylpropionate concentration (Fig. 3) we have calculated the affinity constants corresponding to the sequential binding model NiCPA + β-phenylpropionate $\overset{K_1}{\rightleftharpoons}$ NiCPA(β-phenylpropionate) $\overset{K_2}{\rightleftharpoons}$ NiCPA(β-phenylpropionate)$_2$ as K_1 = (6.0 ± 0.7) × 10^2 and K_2 = (5.5 ± 0.6) × 10^3 dm^3 mol^{-1} (pH 7, 293 K).

The behaviour of phenylacetate is similar to that of β-phenylpropionate, but a greater excess of ligand is required for complete complex formation due to the lesser affinity of phenylacetate. Furthermore, the final ^1H NMR spectrum [Fig. 2(*c*)] is also different from that observed for the β-phenylpropionate complex. The ^1H NMR spectrum of the 1:2 complex [Fig. 2(*c*)] shows three sharp signals at δ 64.6 (a′), 57.1 (d′) and 50.3 (b′, c′), the latter being of double intensity. These signals account for the four protons that are in a *meta*-like position with respect to the metal ion, and so provide evidence that the two histidines are still co-ordinated in the adduct. When the spectrum of the adduct is registered in D_2O the signal at δ 64.6 vanishes completely whereas that at δ 50.3 is reduced to

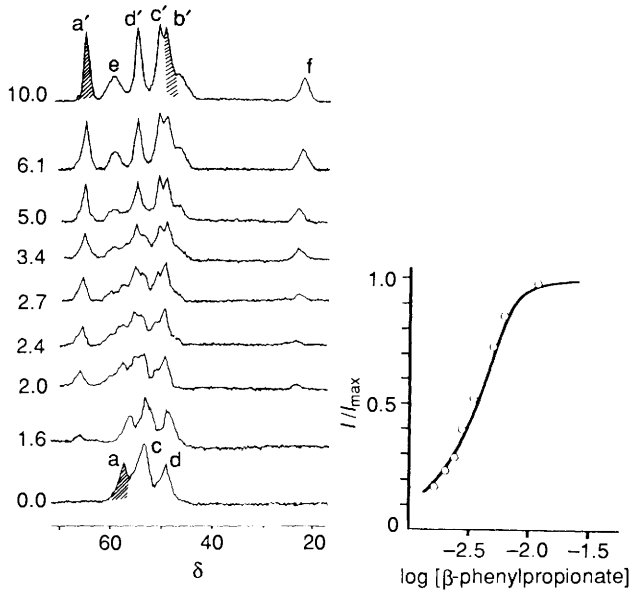

Fig. 3 Proton NMR titration of 2.6 × 10^{-3} mol dm^{-3} NiCPA with increasing concentration (mmol dm^{-3}) of β-phenylpropionate. The relative intensity of signal a′ as a function of increasing β-phenylpropionate concentration is also shown with the best-fitting curve. Other conditions as in Fig. 2

about one-half intensity according to the presence of two exchangeable HN(ε2) protons and two HC(δ2) protons. The spectrum also shows evidence of further broad and barely detectable signals due probably to the HC(ε1) protons of co-ordinated histidines. In contrast to the NiCPA(β-phenylpropionate)$_2$ adduct, no signal is detected at about δ 20 for the phenylacetate adduct.

Titration of NiCPA with up to 3 × 10^{-3} mol dm^{-3} phenylacetate does not affect the ^1H NMR spectrum (Fig. 4). Further increases in concentration, however, induce drastic changes in the spectrum that can be explained by assuming an equilibrium in slow exchange between the 1:1 and 1:2 phenylacetate complexes, as in the case of the β-phenylpropionate complexes. Formation of the NiCPA(phenylacetate)$_2$ complex is complete at a phenylacetate concentration of 0.06 mol dm^{-3} at pH 7. From a best fit of the variation of the normalized area of signal a′ with phenylacetate concentration (Fig. 4), we have calculated the affinity constants as K_1 = (1.0 ± 0.1) × 10^2 and K_2 = (1.2 ± 0.1) × 10^3 dm^3 mol^{-1} (pH 7, 20 °C).

We have also performed a ^1H NMR titration of NiCPA with phenylacetate at pH 8.0. The pattern of signals is similar to that observed at pH 7, and the values of the affinity constants were K_1 = (1.5 ± 0.1) × 10^2 and K_2 = (6.5 ± 0.5) × 10^2 dm^3 mol^{-1}. So, the affinity of phenylacetate for the metal ion decreases at higher pH.

Unlike β-phenylpropionate and phenylacetate, acetate binds NiCPA under fast-exchange conditions on the NMR time-scale and with very low affinity for the metal ion. Furthermore, the ^1H NMR spectrum of the acetate adduct is very different to those of the other adducts, and only one exchangeable NH proton signal is shown. Thus in the presence of 2 mol dm^{-3} acetate, at which the complex is not completely formed, the ^1H NMR spectrum of the adduct displays three resolved signals at δ 63.7 (a′), 55.1 (c′) and 50.0 (d′) as well as a broader one at δ 52.5 [Fig. 2(*b*)]. In D_2O only signal a′ vanishes, allowing it to be assigned to the HN(ε2) of a co-ordinated histidine. The spectrum of the acetate complex is similar to that of NiCPA and the correlation between the signals of both spectra can easily be obtained from a ^1H NMR titration as shown in Fig. 5. The change in shift of signal a′ as a function of acetate concentration is displayed in Fig. 5, and the sigmoidal curve obtained can be fitted by a simple equilibrium of the type

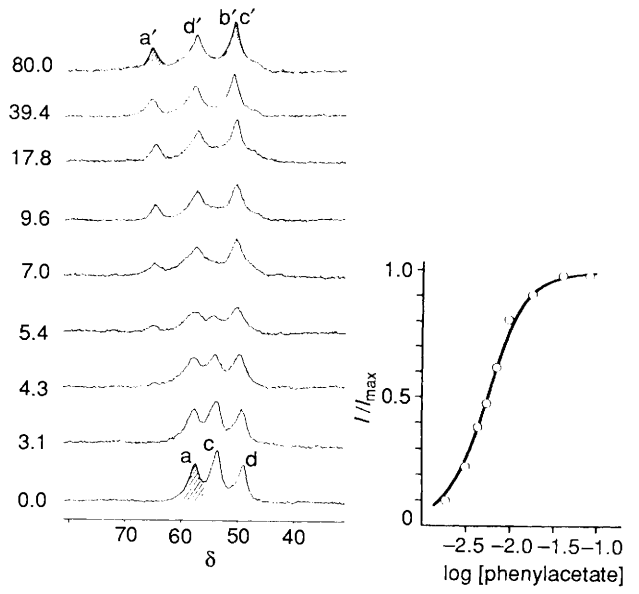

Fig. 4 Proton NMR titration of 2.0×10^{-3} mol dm^{-3} NiCPA with increasing concentration (mmol dm^{-3}) of phenylacetate. The relative intensity of signal a′ *vs.* phenylacetate concentration is also shown. For other conditions see Fig. 2

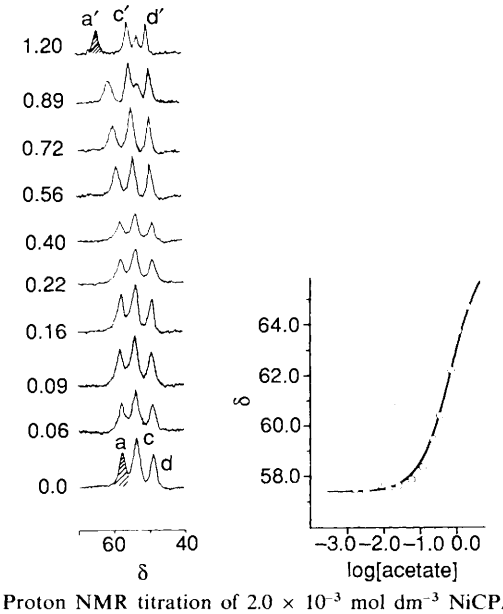

Fig. 5 Proton NMR titration of 2.0×10^{-3} mol dm^{-3} NiCPA with increasing concentration (mol dm^{-3}) of acetate. Variation of chemical shift of signal a′ *vs.* acetate concentration together with the best-fitting curve. Other conditions as in Fig. 2

NiCPA + acetate $\rightleftharpoons$ NiCPA(acetate) with an affinity constant $K_{app} \approx 1$ dm^3 mol^{-1} (pH 7, 20 °C).

We have observed that at the high acetate concentrations required for the complete formation of the acetate complex a remarkable denaturation of the protein is produced. Therefore, the detailed study of this complex is hindered due to its low stability. However the stability of the acetate adduct is very temperature dependent. Indeed, we have also carried out a ^{1}H NMR titration at 10 °C and no denaturation was observed up to 1.5 mol dm^{-3} acetate concentration. The affinity constant obtained was $K_{app} = 3$ dm^3 mol^{-1} (pH 7, 10 °C).

The temperature dependence of the isotropically shifted resonances of the NiCPA(β-phenylpropionate)$_2$ and NiCPA-(phenylacetate)$_2$ complexes has been investigated in the temperature range 5–25 °C. In Fig. 6 the observed isotropic shifts

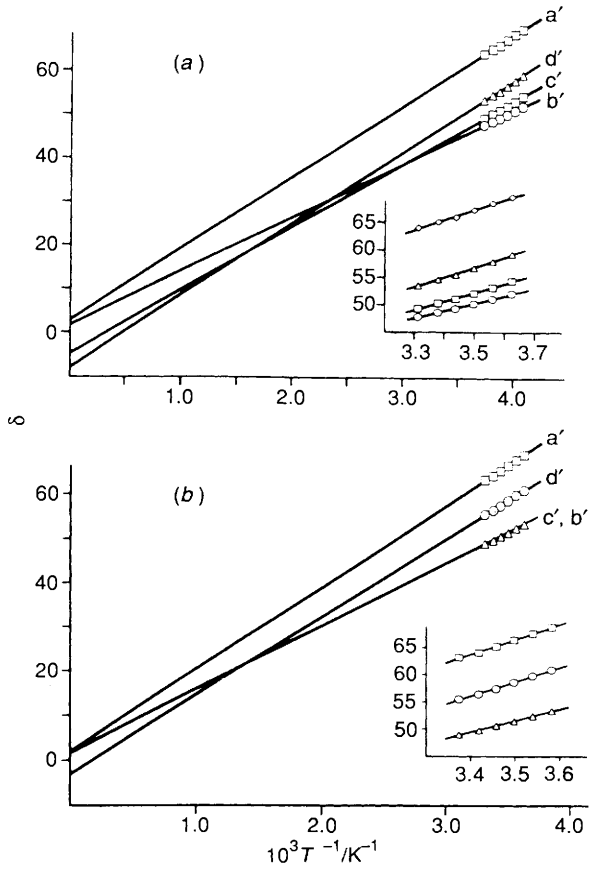

Fig. 6 Temperature dependence of the isotropic shifts for NiCPA adducts at pH 7: (*a*) NiCPA(β-phenylpropionate)$_2$, (*b*) NiCPA(phenylacetate)$_2$

of the HN(ε2) and HC(δ2) protons are plotted *vs.* T^{-1}. All the signals follow a Curie-like behaviour, *i.e.* their isotropic shifts decrease with increasing temperature. The intercept values at infinite temperature were within or close to the diamagnetic region. Thus, the results indicate little dipolar contribution to the isotropic shifts in both complexes, though it is more appreciable in the β-phenylpropionate complex [Fig. 6(*a*)]. The spread of the ^{1}H NMR signals (Fig. 2) as well as their longitudinal relaxation times (Table 1) are also consistent with larger magnetic anisotropy in the latter complex.

The T_1 values of the protons of co-ordinated histidines are in Table 1. The values are between 2 and 6.5 ms for the 1:2 complexes whereas the NiCPA shows $T_1 \leqslant 1$ ms.

Assignments by ^{1}H *NOE Experiments.*—The NOEs in large paramagnetic biomolecules are relatively difficult to observe due to the short nuclear relaxation times which decrease the NOEs in comparison to analogous diamagnetic systems.[36,37] On the other hand, NOE measurements might provide information on the interproton distances and add further information about the structure of the metal co-ordination polyhedron. Therefore, NOE experiments constitute a powerful method for obtaining structural information and, in addition, this technique is becoming preferred for resonance assignments.[38] The NOE, η_{ij}, for a proton i is defined as the fractional variation in intensity of signal i upon saturation of the resonance of another proton j in the same molecular species. It is dependent on the time t of irradiation of signal j, but for long irradiation times ($t \gg \rho_i^{-1}$), the steady state is reached, where the NOE is maximal and η_{ij} is given by equation (3). Here σ_{ij} is

$$\eta_{ij} = \frac{\sigma_{ij}}{\rho_i} = -\frac{\hbar^2\gamma^4\tau_c}{10\,\rho_i r_{ij}^6} \qquad (3)$$

Table 1 Proton NMR (200 MHz) chemical shifts (δ) and T_1/ms (in parentheses) values for nickel-substituted carboxypeptidase and its adducts at pH 7 and 20 °C

	NiCPA	NiCPA(β-phenylpropionate)$_2$	NiCPA(phenylacetate)$_2$	NiCPA(acetate)
a(NH-69)	57.5 (< 1)	65.6 (2.7)	64.6 (2)	63.7
b(NH-196)	—	49.0 (4.3)	50.3 (2.6)	—
c(CH-69)	53.3 (< 1)	50.8 (6.4)	50.3 (2.6)	55.1
d(CH-196)	48.9	55.1 (3.2)	57.1 (2.5)	50.0
e(γ-CH_2-72)	—	60 (*ca.* 1)	—	—
f(γ-CH_2-72)	—	22	—	—

Table 2 Steady-state NOE measured between the isotropically shifted resonances of the NiCPA(β-phenylpropionate)$_2$ complex. The data were recorded at 200 MHz and 25 °C and are reported as the percentage decrease in signal intensity. The calculated distances (Å) are in parentheses

	Observed peak			
Saturated peak	a′	b′	c′	e
a′			4.5 (2.2)	
c′	1.9 (2.2)			
d′		2.3 (2.3)		
f				7 (1.5)

the cross-relaxation rate between protons i and j, ρ_i is the selective spin–lattice relaxation rate of proton i, τ_c is the reorientation time of the vector connecting H_i and H_j, and r_{ij} is the interproton distance. The overall correlation time τ_c for a macromolecule can be estimated by the Stokes–Einstein relationship[39] $\tau_c = 4\pi\zeta a^3/3kT$ where a is the molecular radius and ζ the viscosity of the solvent.

Recently, the effectiveness of the different NOE experiments in the general case of paramagnetic macromolecules was analysed, and it was concluded that steady-state NOE provides better results from the qualitative and quantitative points of view.[40] We performed ^{1}H NOE experiments to assign the paramagnetically resolved signals of the complex NiCPA-(β-phenylpropionate)$_2$. The difference spectra obtained upon saturating the shifted resonances are shown in Fig. 7. Saturation of signals a′ and d′ induces NOEs greater than 2% in peaks c′ and b′ respectively. The a′–c′ and b′–d′ correlations were checked by saturating signals c′ and b′ which yielded NOEs in peaks a′ and d′ respectively. Furthermore, the relatively broad signals e and f are also correlated through NOE. All the NOE values are reported in Table 2 as a percentage of the irradiated peak intensity. By using equation (3), with a τ_c value of 1.4×10^{-8} s, as calculated by the Stokes–Einstein equation, we determined interproton distances of 2.2 ± 0.2 and 2.3 ± 0.2 Å for the a′–c′ and b′–d′ pairs of protons. These distances are consistent with the above pairs of protons being vicinal protons in the imidazole ring [HN(ε2), HC(δ2)] of each of the co-ordinated histidines.

Though a precise determination of the T_1 values of signals e and f was not possible due to the short relaxation times of these signals, we have estimated that the T_1 value of signal e was about 1 ms. It should be noted that a factor of two in T_1 gives a 10% difference in distances. Despite this short T_1 value, saturation of signal f gives rise to a strong NOE in peak e indicating that this pair of protons is spatially very near as occurs for geminal protons. The calculated distance for the e–f pair of protons was $r_{ef} = 1.5 \pm 0.2$ Å which is consistent with e and f being geminal protons of a CH_2 group.

^{13}C NMR Relaxation Rates.—Carbon-13 NMR T_1 and T_2 measurements have been performed for ^{13}C-enriched-carboxylate phenylacetate and acetate inhibitors in the presence of nickel(II) carboxypeptidase. The relaxation rates T_1^{-1} and T_2^{-1} for the carboxylate groups of both inhibitors are drastically

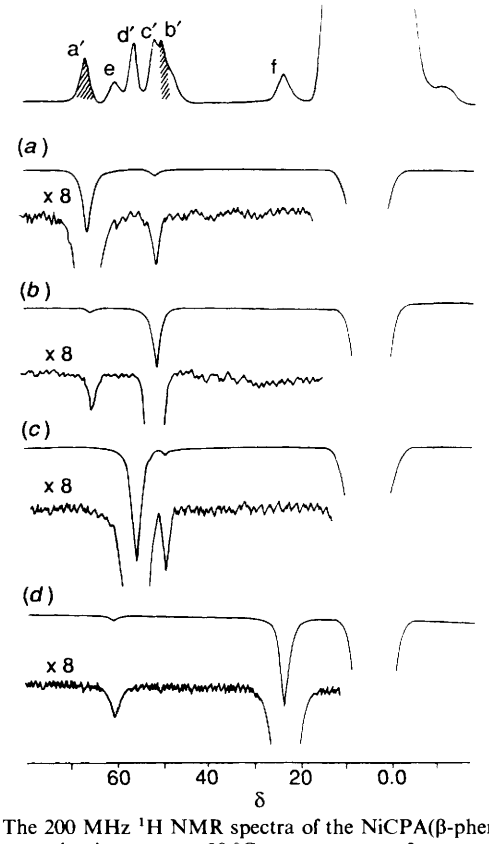

Fig. 7 The 200 MHz ^{1}H NMR spectra of the NiCPA(β-phenylpropionate)$_2$ complex in water at 20 °C: upper trace, reference spectrum; traces (*a*)–(*d*) show steady-state NOE difference spectra obtained by saturating peaks a′, c′, d′ and f respectively. Solution conditions: 4.0×10^{-3} mol dm^{-3} NiCPA, 15×10^{-3} mol dm^{-3} β-phenylpropionate, pH 7

increased when bound to the paramagnetic nickel derivative as compared to the diamagnetic native enzyme. The relaxation-rate enhancement can be attributed to dipolar coupling of the ^{13}C nucleus with the paramagnetic nickel ion, and thus can be used to calculate the M ··· ^{13}C nucleus distance in the adduct. However, rapid exchange of the ligand must occur in order to relate the observed relaxation-rate enhancements to the relaxation parameters of the bound ligand.

In Fig. 8 the ^{13}C NMR T_2^{-1} values are plotted against the logarithm of phenylacetate concentration. The best fit of the experimental data gave $K_1 = 3 \times 10^2$ and $K_2 = 5 \times 10^2$ dm^3 mol^{-1} (pH 8, 20 °C), of the same order of magnitude found through ^{1}H NMR spectroscopy. As previously indicated, upon binding, the second phenylacetate molecule enters a slow-exchange regime on the chemical shift time-scale. Therefore, the ^{13}C T_2^{-1} values probably reflect some exchange-controlled line broadening. Thus, in order to avoid these interferences we prefer to work with T_1^{-1} measurements. The fact that T_{2p}^{-1} values are about one order of magnitude higher than T_{1p}^{-1} ensures that the latter are in the fast-exchange regime and thus can be used for calculations of M ··· ^{13}C distance by using the Solomon

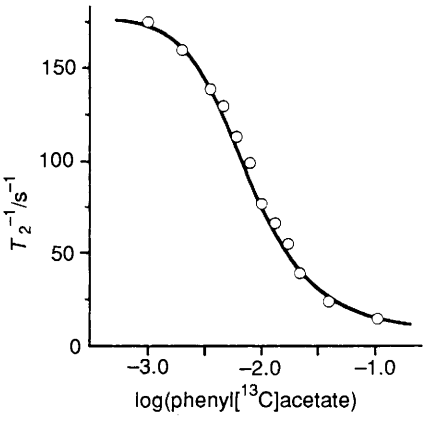

Fig. 8 Dependence of ^{13}C T_2^{-1} values for NiCPA at pH 7 on the presence of increasing amounts of $^{13}CO_2^-$-enriched phenylacetate. Solution conditions: 1×10^{-3} mol dm^{-3} NiCPA, 20 °C

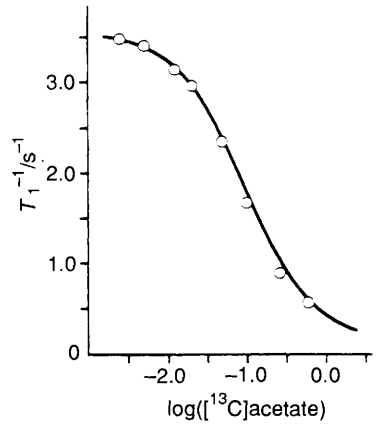

Fig. 9 Values of T_1^{-1} for the ^{13}C nucleus as a function of $^{13}CO_2^-$-enriched acetate concentration in the presence of 0.8×10^{-3} mol dm^{-3} NiCPA. Solution conditions are 10 °C and pH 7 (0.05 mol dm^{-3} hepes, 1 mol dm^{-3} NaCl)

equation[41] (5), where μ_0 is the permeability of a vacuum, γ_n is the nuclear magnetogyric ratio, g_e is the electron g factor, τ_s is the electronic relaxation time, ω_I is the nuclear Larmor frequency and ω_s is the electronic Larmor frequency.

$$T_{1M}^{-1} = (2/15)(\mu_0/4\pi)^2 \frac{\gamma_n^2 g_e^2 \mu_B^2 S(S+1)}{r^6} \times \left(\frac{7\tau_s}{1+\omega_s^2\tau_s^2} + \frac{3\tau_s}{1+\omega_I^2\tau_s^2}\right) \quad (5)$$

We have performed T_1 ^{13}C NMR measurements on 15×10^{-3} mol dm^{-3} phenylacetate, ^{13}C enriched at the carboxylate, in the presence of 0.8 mmol dm^{-3} NiCPA at pH 8. Under these conditions the 1:2 complex is the predominant species ($\alpha_1 = 0.1$, $\alpha_2 = 0.85$). By using equation (2), $T_{1M(2)}^{-1}$ was calculated as 192 s^{-1}. By taking a τ_s value of 1×10^{-11} s,[42] and through use of the Solomon equation, a Ni^{II} ··· ^{13}C distance of 3.0 ± 0.2 Å was determined. The distance is consistent with direct co-ordination of the second phenylacetate molecule to the metal ion. Similarly, ^{13}C NMR T_1 measurements were performed for ^{13}C-enriched acetate in the presence of NiCPA at pH 7. As T_1 experiments, at low acetate concentrations, are time-consuming, the study was made at 10 °C in order to avoid denaturation of the protein. In Fig. 9 the ^{13}C NMR T_1^{-1} values are plotted as a function of the inhibitor concentration. The best fit of the experimental values gave $T_{1M}^{-1} = 315$ s^{-1} and $K_{app} = 9$ dm^3 mol^{-1}. The latter value is consistent with that found by ^1H NMR titrations. By using equation (5), with $\tau_s = 5 \times 10^{-11}$ s,[42,43] a Ni^{II} ··· ^{13}C distance of 2.7 ± 0.3 Å was obtained, indicative of direct co-ordination of the acetate to the nickel ion.

Discussion

Nickel(II) carboxypeptidase interacts with the carboxylates β-phenylpropionate and phenylacetate forming two complexes of stoichiometries 1:1 and 1:2. Whereas the first inhibitor molecule binds at a non-metallic site, the second binds directly to the metal ion. Indeed, the ^1H NMR titrations of NiCPA with these carboxylates show that binding of the second equivalent induces drastic changes in the ^1H NMR and electronic absorption spectra. Moreover, the Ni ··· $^{13}CO_2^-$ distance of *ca.* 3.0 Å calculated from the ^{13}C NMR T_1 value for the second phenylacetate molecule indicates that the carboxylate group of the latter binds directly to the metal ion.

Phenylacetate and β-phenylpropionate exhibit multiple modes of inhibition toward carboxypeptidase catalysis of peptide hydrolysis and the type of inhibition varies with pH.[44] The influence of pH on the resolved inhibition components has shown that the observed mixed inhibition could be due to the binding of the inhibitor in two different modes.[45] Our results for the binding of β-phenylpropionate and phenylacetate to NiCPA are in agreement with these kinetic data. Moreover, multiple binding modes for these molecules have been well established, through electronic absorption, CD, NMR and EPR studies of the active cobalt enzyme.[18,19,46] Thus, at low concentration these inhibitors act non-competitively toward peptide hydrolysis and alter the CoCPA absorption spectrum only slightly, while at high concentrations they act competitively and have a more marked effect on the visible absorption spectrum.

The affinity constants of β-phenylpropionate and phenylacetate for the metal binding to NiCPA are significantly greater than for the native enzyme where the K values are respectively $\approx 10^3$ (at pH 6) and 10^2 dm^3 mol^{-1}.[45,47] As already reported, the amino acids L- and D-phenylalanine also show higher affinity for the nickel enzyme.[23] On the other hand, at pH 8 the affinity for the binding of the second phenylacetate molecule to NiCPA is less than at neutral pH. This behaviour would be as expected if the inhibitor binds most tightly to the EH_2 form of the enzyme as has been proposed.[44] In this context, the determined affinity constant at pH 7 for the metal binding of β-phenylpropionate, $K_2 = 5.5 \times 10^3$ dm^3 mol^{-1}, is nicely consistent with that already found at pH 7.8, $K = 3.7 \times 10^3$ dm^3 mol^{-1}, by spectrophotometric measurements.[35]

The electronic absorption spectra of the 1:2 phenylacetate and β-phenylpropionate complexes are very similar. On the basis of both the position and intensity of the absorption bands the spectrum of the latter complex was interpreted as being due to five-co-ordination.[35] The ^1H T_1 values of the co-ordinated histidines can provide additional information about the nickel co-ordination geometry. Such data for nickel(II) metalloproteins are very scarce, however T_1 values for the adducts of nickel(II)-substituted carbonic anhydrase with several anions have recently been reported.[11,12] It has been proposed that the nickel ion is five-co-ordinated in these adducts and their ^1H T_1 values were between 2 and 10 ms for the *m*-protons of the co-ordinated histidines. For the NiCPA(L)$_2$ complexes (L = β-phenylpropionate or phenylacetate) the T_1 values are between 2 and 6.5 ms and so they would be consistent with a five-co-ordinated stereochemistry for the nickel ion and in accord with the analysis of their electronic spectra.

The ^1H NMR spectra of the 1:2 adducts indicate that two histidines are co-ordinated to the metal ion as in the nickel enzyme. Indeed, ^1H NOE experiments on the β-phenylpropionate complex have allowed us to assign the four sharp ^1H NMR signals to the co-ordinated histidines, His-69 and -196. However, binding of the carboxylate to the metal ion produces marked changes in the positions of the shifted proton

signals, indicating that the co-ordinated histidines change their spatial arrangement around the metal ion. For the 1:2 complexes the ligands undergo slow exchange on the chemical shift time-scale. It would appear that binding of the second carboxylate molecule induces some conformational change which retards the overall exchange process. As a consequence, the NH of the His-196 probably will be less exposed to solvent and undergoes slower exchange, thus allowing its ^{1}H NMR detection.

In contrast to the carboxylate inhibitors described above, acetate shows no evidence for more than a single binding mode to the nickel enzyme. Thus, the present ^{1}H and ^{13}C NMR data reveal that acetate only forms a 1:1 complex with NiCPA in the fast-exchange regime. Moreover, the $Ni^{II} \cdots {}^{13}CO_2^-$ distance calculated by means of the Solomon equation indicates that the ligand is directly co-ordinated to the metal ion.

The ^{1}H NMR spectrum of the acetate adduct, NiCPA-(acetate), shows the same pattern as the spectrum of the nickel enzyme. However, as observed in Fig. 5, upon binding of acetate the signals a′ and c′ assigned to His-69[23] change their chemical shift, the latter signal to a lesser extent, while signal d′ assigned to His-196 remains virtually unchanged. Therefore His-69 probably changes slightly its spatial arrangement when the complex is formed, whereas His-196 remains in the same orientation. On the other hand, in the case of the cobalt carboxypeptidase, it has been proposed that acetate binds at two distinct sites.[18] Indeed, from the ^{13}C line-broadening measurements at acetate concentrations lower than 10^{-2} mol dm^{-3} the existence of a non-metallic binding site of high affinity (> 500 dm^3 mol^{-1}) for this ligand has been suggested.[18] Although the existence of an additional non-metallic site for acetate could not be ruled out, under the present experimental conditions our ^{13}C T_1 measurements do not provide any evidence for such a site.

Finally, the exchangeable signal a′ is shifted the most downfield in the ^{1}H NMR spectra of all the carboxylate complexes as well as in NiCPA. Signal a for the nickel enzyme has been assigned to the NH(ε2) of the co-ordinated histidine, His-69.[23] Consequently, the same assignment can be made for signal a′ of the acetate adduct, in accord with the correlations established through ^{1}H NMR titrations. Since signal a′ occurs practically at the same position for all carboxylate adducts (δ 64.5 ± 1), it is reasonable to assume that this NH signal belongs to the same histidine, His-69. In the β-phenylpropionate complex signal a′ is connected to c′ through NOE and the obtained distance agrees with signal c′ being due to HC(δ2) of His-69. Analogously, the interproton distance evaluated for the b′–d′ protons is consistent with signals b′ and d′ being HC(δ2) and NH(ε2), respectively, of His-196.

In addition, ^{1}H NOEs have been detected for geminal protons (signals e and f), owing to their short reciprocal distances (≈ 1.7 Å) despite the short T_1. These signals may have originated from a γ-CH_2 group of the Glu-72 ligand. The assignment of the γ-CH_2 protons of glutamic residues constitutes a classic problem in the NMR spectroscopy of paramagnetic proteins. It has been reported that the spin-delocalization mechanisms would give remarkable downfield isotropic shifts for a CH_2 group in the case of bidentate carboxylate co-ordination.[48–50] However, monodentate co-ordination would give rise to moderate downfield shifts. Therefore, our results would favour the assignment of the signals at δ 60 and 22 to γ-CH_2 protons of a bidentate Glu-72.

Acknowledgements

We thank the CICYT (Ministerio de Educación y Ciencia, Spain) for its financial support of this work (Proyecto No. PB 88-0489). We are indebted to Professor I. Bertini at Florence University for many helpful discussions.

References

1 B. L. Vallee, A. Galdes, D. S. Auld and J. F. Riordan, in *Zinc Enzymes, Metal Ions in Biology*, ed. T. G. Spiro, Wiley-Interscience, New York, 1983, vol. 5, pp. 26–75.
2 D. S. Auld, J. F. Riordan and B. L. Vallee, in *Metal Ions in Biological Systems*, ed. H. Sigel, Marcel Dekker, New York, 1989, vol. 25, pp. 359–393.
3 S. Mobashery, S. S. Ghosh, S. S. Tamura and E. T. Kaiser, *Proc. Natl. Acad. Sci. USA*, 1990, **87**, 578.
4 D. W. Christianson and W. N. Lipscomb, *J. Am. Chem. Soc.*, 1988, **110**, 5560.
5 M. T. Martin, B. Holmquist and J. F. Riordan, *J. Inorg. Biochem.*, 1989, **36**, 39.
6 D. H. Kim and K. B. Kim, *J. Am. Chem. Soc.*, 1991, **113**, 3200.
7 D. C. Rees, M. Lewis and W. N. Lipscomb, *J. Mol. Biol.*, 1983, **169**, 369.
8 D. S. Auld and B. L. Vallee, in *Hydrolytic Enzymes*, eds. A. Neuberger and K. Brockjehurst, Elsevier, New York, 1987, pp. 201–255.
9 Y. Pocker, in *Metal Ions in Biological Systems*, ed. H. Sigel, Marcel Dekker, New York, 1989, vol. 25, p. 335.
10 I. Bertini and C. Luchinat, *NMR of Paramagnetic Molecules in Biological Systems*, Benjamin Cummings, Boston, 1986.
11 J. M. Moratal, M. J. Martinez-Ferrer, A. Donaire, J. Castells, J. Salgado and H. R. Jiménez, *J. Chem. Soc., Dalton Trans.*, 1991, 3393.
12 J. M. Moratal, M. J. Martinez-Ferrer, H. R. Jiménez, A. Donaire, J. Castells and J. Salgado, *J. Inorg. Biochem.*, 1992, **45**, 231.
13 M. D. Bond, B. Holmquist and B. L. Vallee, *J. Inorg. Biochem.*, 1986, **28**, 97.
14 K. D. Hardman and W. N. Lipscomb, *J. Am. Chem. Soc.*, 1984, **106**, 463.
15 R. Bicknell, A. Schäffer, I. Bertini, C. Luchinat, B. L. Vallee and D. S. Auld, *Biochemistry*, 1988, **27**, 1050.
16 I. Bertini, C. Luchinat, L. Messori, R. Monnanni, D. S. Auld and J. F. Riordan, *Biochemistry*, 1988, **27**, 8318.
17 C. Luchinat, R. Monnanni, S. Roelens, B. L. Vallee and D. S. Auld, *J. Inorg. Biochem.*, 1988, **32**, 1.
18 I. Bertini, R. Monnanni, G. C. Pellacani, M. Sola, B. L. Vallee and D. S. Auld, *J. Inorg. Biochem.*, 1988, **32**, 13.
19 R. A. Martinelli, G. R. Hanson, J. S. Thompson, B. Holmquist, J. R. Pilbrow, D. S. Auld and B. L. Vallee, *Biochemistry*, 1989, **28**, 2251.
20 D. Christianson and W. N. Lipscomb, *J. Am. Chem. Soc.*, 1986, **108**, 545.
21 D. Christianson and W. N. Lipscomb, in *Zinc Enzymes*, eds. I. Bertini, C. Luchinat, W. Maret and M. Zeppezuer, Birkhauser, Boston, 1986, p. 121.
22 D. W. Christianson, S. Mangani, G. Shoham and W. N. Lipscomb, *J. Biol. Chem.*, 1989, **264**, 12849.
23 I. Bertini, A. Donaire, R. Monnanni, J. M. Moratal and J. Salgado, *J. Chem. Soc., Dalton Trans.*, 1992, 1443.
24 J. M. Moratal, A. Donaire, J. Castells, H. R. Jiménez, J. Salgado and F. Hillerns, *J. Chem. Soc., Dalton Trans.*, 1992, 713.
25 D. J. Cox, F. C. Bovard, A. Bargetzi, K. A. Walsh and H. Neurath, *Biochemistry*, 1964, **3**, 44.
26 R. Bicknell, A. Schaffer, D. S. Auld, J. F. Riordan, R. Monnanni and I. Bertini, *Biochem. Biophys. Res. Commun.*, 1985, **133**, 787.
27 T. J. Bazzone, M. Sokolovsky, L. B. Cueni and B. L. Vallee, *Biochemistry*, 1979, **18**, 4362.
28 D. S. Auld and B. Holmquist, *Biochemistry*, 1974, **13**, 4355.
29 M. D. Bond, B. Holmquist and B. L. Vallee, *J. Inorg. Biochem.*, 1986, **28**, 97.
30 R. E. Thiers, in *Methods of Biochemical Analysis*, ed. D. Glick, Interscience, New York, 1955, vol. 5, pp. 273–335.
31 R. T. Simpson, J. F. Riordan and B. L. Vallee, *Biochemistry*, 1963, **2**, 616.
32 T. Inubushi and E. D. Becker, *J. Magn. Reson.*, 1983, **51**, 128.
33 J. Hockmann and H. Kellerhals, *J. Magn. Reson.*, 1980, **38**, 23.
34 L. Banci, I. Bertini, C. Luchinat, M. Piccioli and A. Scozzafava, *Inorg. Chem.*, 1989, **28**, 4650.
35 R. C. Rosenberg, C. A. Root and H. B. Gray, *J. Am. Chem. Soc.*, 1975, **97**, 21.
36 L. Banci, I. Bertini, C. Luchinat, M. Piccioli and A. Scozzafava, *Inorg. Chem.*, 1989, **28**, 4650.
37 L. B. Dugad, G. N. La Mar and S. W. Unger, *J. Am. Chem. Soc.*, 1990, **112**, 1386.
38 J. D. Satterlee, in *Metal Ions in Biological Systems*, ed. H. Sigel, Marcel Dekker, New York, 1987, vol. 21, p. 121.

39 J. H. Noggle and R. E. Shirmer, *The Nuclear Overhauser Effect*, Academic Press, New York, 1971.
40 L. Banci, I. Bertini, C. Luchinat and M. Piccioli, *FEBS Lett.*, 1990, **272**, 175.
41 I. Solomon, *Phys. Rev.*, 1955, **99**, 559.
42 I. Bertini, in *Magneto-Structural Correlation in Exchange Coupled Systems*, eds. R. D. Willet, D. Gatteschi and O. Kahn, Riedel, Dordrecht, 1985, p. 443.
43 F. Hirata, H. L. Friedman, M. Holz and H. G. Hertz, *J. Chem. Phys.*, 1980, **73**, 6031.
44 D. S. Auld, K. Larson and B. L. Vallee, in *Zinc Enzymes*, eds. I. Bertini, C. Luchinat, W. Maret and M. Zeppezauer, Birkhäuser, Stuttgart, 1986, p. 133.
45 D. S. Auld, K. Geoghegan, A. Galdes and B. L. Vallee, *Biochemistry*, 1986, **25**, 5156.
46 S. A. Latt and B. L. Vallee, *Biochemistry*, 1971, **10**, 4263.
47 D. S. Auld, S. A. Latt and B. L. Vallee, *Biochemistry*, 1972, **11**, 4994.
48 I. M. Arafa, H. M. Goff, S. S. David, B. P. Murch and L. Que, jun., *Inorg. Chem.*, 1987, **26**, 2779.
49 R. H. Holm and C. J. Hawkins, in *NMR of Paramagnetic Molecules*, eds. G. N. La Mar, W. D. Horrocks and R. H. Holm, Academic Press, New York, 1973, pp. 243–332.
50 L. J. Ming, L. Banci, C. Luchinat, I. Bertini and J. S. Valentine, *Inorg. Chem.*, 1988, **27**, 4458.

Received 5*th June* 1992; *Paper* 2/02992H